Available online at www.sciencedirect.com
SCIENCE DIRECT®
ELSEVIER
Talanta 67 (2005) 730–735
Talanta
www.elsevier.com/locate/talanta

Mercury transformations in chemical agent simulant as characterized by X-ray absorption fine spectroscopy

Laura R. Skubal[a,*], Sandra G. Biedron[a], Matthew Newville[b], John F. Schneider[a],
Stephen V. Milton[a], Piero Pianetta[c], H. Jack O'Neill[a]

[a] Argonne National Laboratory, 9700 South Cass Avenue, Argonne, IL 60439, USA
[b] Consortium for Advanced Radiation Science, The University of Chicago, 9700 South Cass Avenue, Argonne, IL 60439-4815, USA
[c] Stanford Synchrotron Radiation Laboratory, Stanford Linear Accelerator Center, 2575 Sand Hill Road, MS 69, Menlo Park, CA 94025-7015, USA

Received 22 December 2004; received in revised form 23 March 2005; accepted 24 March 2005

Abstract

Chemical analyses of U.S. stockpiled mustard chemical warfare agent show some agent destined for destruction contains mercury [L. Ember, Chem. Eng. News 82 (2004) 8]. Because of its toxicity, mercury must be removed from agent prior to incineration or be scrubbed from incineration exhaust to prevent release into the atmosphere. Understanding mercury/agent interactions is critical if either atmospheric or aqueous treatment processes are used. We investigate and compare the state of mercury in water to that in thiodiglycol, a mustard simulant, as co-contaminants are introduced. The effects of sodium hypochlorite and sodium hydroxide, common neutralization chemicals, on mercury in water and simulant with and without co-contaminants present are examined using X-ray absorption fine spectroscopy (XAFS).

Keywords: Mercury; Thiodiglycol; XAFS; Chemical warfare agent simulant; Mustard

1. Introduction

One of the fundamental doctrines of the *Chemical Weapons Convention* [2] is the non-proliferation of chemical weapons and their precursors. Several facilities in the U.S. are capable of destroying stockpiled agent using two common methods: incineration and chemical destruction. Chemical destruction processes rely on caustic addition to agent, essentially "neutralizing" the agent by hydrolysis. Incineration processes thermally convert neutralized agent to lesser organics. If incineration processes are to be used, then the neutralized aqueous waste sent to the incinerator must be free of contaminants including metal impurities added during the manufacturing processes that could potentially pose an air quality problem [3]. It is believed that approximately 1600 1-ton containers in the U.S. holding mustard agent, bis(2-chloroethyl) sulfide, contain elevated concentrations of mercury, possibly as a result of the containers having previously been used for delivering mercuric chloride for other military production processes without having been cleaned thoroughly before agent storage [1]. Many containers housing stockpiled agent have incomplete histories, as cradle-to-grave concepts were not implemented when the nation's chemical agent stockpiles were established, which further complicates efforts to characterize their contents. Analysis of agent also is made difficult by the toxicity of both raw waste and treated hydrolysate, which limits waste transport, handling, and analysis.

Various accepted and experimental waste treatment processes, including precipitation, co-precipitation, ion exchange, electrochemical operations, solvent extraction, membrane separation, adsorption, microbial reduction and retention, and evaporation are effective at removing metals

---

* Corresponding author. Tel.: +1 630 252 0931; fax: +1 630 252 6407.
E-mail address: lskubal@anl.gov (L.R. Skubal).

0039-9140/$ – see front matter © 2005 Elsevier B.V. All rights reserved.
doi:10.1016/j.talanta.2005.03.030

from well-characterized aqueous waste streams [4–6]. Incineration of solutions containing residual metals, particularly mercury, can convert the metals from an aqueous state to a gaseous state, posing an air pollution issue. A number of tools are commonly used to scrub mercury from industrial combustion exhaust gases. These include electrostatic precipitators, fabric filters, venturi particulate scrubbers, wet scrubbers, deep bed carbon adsorbers, and selenium filters [7,8]. Although no single technology can be applied broadly, combinations of control methods can be as much as 90% effective in removing mercury from stack emissions. However, studies at coal-fired power plants show that more typical mercury removal efficiencies are on the order of 40% [8]. Process efficiency depends upon comprehensive characterization of mercury content and speciation in the original liquid waste and in the gas phase.

If mercury is present at high concentrations in a liquid waste, it is oftentimes easier to remove the mercury from the aqueous state rather than to scrub it from the gas phase if the waste is destined for incineration. Aqueous-phase mercury can exist in one of three oxidation states: as the free metal, Hg^o; as the mercurous ion, ${Hg_2}^{2+}$; or as the mercuric ion, Hg^{2+} [9]. Several recent studies have used X-ray absorption fine spectroscopy (XAFS) techniques to evaluate the fate and equilibrium state of aqueous mercury in various oxides, sorbents, and substrates. These studies, using the Hg L_{III}-edge, have shown that XAFS techniques are non-destructive, relatively sensitive at low concentrations, require minimal sample preparation needs, and able to provide local structural information around the mercury atom, establishing the relative proportions of major Hg phases in a sample [10–13].

The determination of mercury contamination in ton containers holding liquid mustard agent has previously been performed using techniques such as X-ray fluorescence, without analytical determination of the oxidation state of mercury in the agent. However, speciation information is essential for maximizing the efficiency of air pollution devices removing mercury from incineration exhaust or for developing direct aqueous mercury removal processes. This study for the first time identifies mercury speciation in a mustard agent simulant. Simulant was used, since the facility where the work was performed (the Advanced Photon Source) does not have certification to allow the probing or storage of neat chemical agents. Specific objectives of the study include: (1) examining the initial state of mercury after equilibration with the mustard agent simulant, thiodiglycol (bis(2-hydroxyethyl) sulfide); (2) determining the state of mercury in thiodiglycol hydrolysates produced with sodium hypochlorite or with a sodium hypochlorite and sodium hydroxide mixture, added to mimic agent deactivation; (3) comparing mercury speciation in water and thiodiglycol; and (4) identifying the effect on mercury speciation by ions that commonly co-contaminate mustard agent in ton containers, e.g., arsenic, cadmium, iron, and selenium. XAFS, particularly X-ray absorption near edge spectroscopy (XANES), is used to characterize the solutions.

2. Experimental

Concentrated stock solutions of metals including mercuric chloride ($HgCl_2$), cadmium chloride ($CdCl_2$), ferrous sulfate ($FeSO_4$), ferric oxide (Fe_2O_3), arsenic trioxide (As_2O_3), and selenious acid (H_2SeO_3) (all purchased from Aldrich) were prepared in distilled water. Aliquots of the stock metal solutions were added to both distilled water and to thiodiglycol ($C_4H_{10}O_2S$) to yield metal concentrations that were expected to simulate levels present in ton containers storing mustard agent. Blanks were prepared using only distilled water and mustard simulant (thiodiglycol). Eight-milliliter aliquots of each solution were individually transferred to X-ray fluorescence (XRF) cups (Chemplex Industries Inc.), covered with Kapton film, and equilibrated in the dark at ambient temperatures for 10 months. This extended equilibration period was used to emulate the extended contact time between mustard agent and mercury in ton containers. After the equilibration period, samples were opened and divided. Four milliliters of each sample were transferred to new XRF cups and covered with Kapton film, and 4 mL of each sample were "neutralized" with 5.25% sodium hypochlorite (NaOCl, Clorox), transferred to new XRF cups, and covered with Kapton film. The state of mercury in the samples was determined using XAFS at the Argonne National Laboratory Advanced Photon Source GSECARS Beamline 13BM. Samples were positioned at 45° to the beam. The XAFS spectra were recorded in fluorescence mode as a function of incident X-ray energy from a water-cooled Si(1 1 1) monochromator by measuring the integrated Hg L_α fluorescence intensity using a 16-element Ge detector placed in the horizontal plane, along the polarization vector of the synchrotron radiation [14].

Samples containing sodium hypochlorite were neutralized again with sodium hydroxide (NaOH) (from Aldrich) and reanalyzed to determine the state of mercury. Table 1 lists the samples prepared and analyzed.

3. Results and discussion

Fig. 1 shows the XAFS spectra for various mercury-containing compounds including HgO, HgSCN, HgS (black), and $HgCl_2$. These spectra are provided for those not familiar with XAFS, and show differences between the unique mercury compounds. The sample compositions reported hereafter are based on linear combinations of these standards, have a typical uncertainty of 10%, and should be interpreted more as a *suggestion* of speciation and as a way to compare two spectra than as a precise assignment of sample composition. That is, while the spectral signatures for Hg–Cl, Hg–O, and Hg–S ligands are distinctive, the XAFS spectra also can be influenced by changes in coordination chemistry that may not be fully represented in the model compounds used for the linear combinations.

Figs. 2–5 show the samples' Hg L_{III}-edge XAFS spectra. Specifically, Fig. 2 compares Hg speciation in water and

Table 1
Composition of solutions prepared for analysis

Distilled water	Thiodiglycol	1000 ppm Hg from $HgCl_2$	1000 ppm Fe from $FeSO_4$	1000 ppm Fe from Fe_2O_3	100 ppm Cd from $CdCl_2$	100 ppm Se from H_2SeO_3	150 ppm As from As_2O_3	Sample number[a]
×		×						06
	×	×						04 b,bc
×		×		×				16
	×	×		×				15 b,bc
×		×		×			×	17
	×	×		×			×	14 b,bc
	×	×	×					05
	×	×	×		×			19
		×	×		×	×		07
	×	×		×	×			22 b,bc
	×	×		×	×	×		23 b,bc
	×	×		×	×		×	24 b,bc
	×	×					×	25 b,bc
	×	×		×	×	×	×	26 b,bc

[a] *Note*: Samples containing a "b" denote that the sample was split, NaOCl was added (resultant concentration of 0.04 M), and both solutions were analyzed. "bc" denotes NaOH was added (resultant concentration of 0.2 M) to the sample containing NaOCl, and solution was analyzed again.

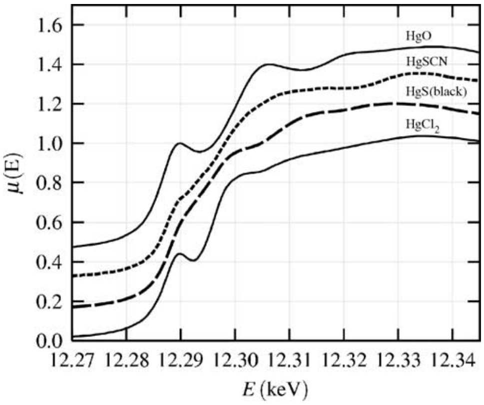

Fig. 1. Hg L_{III} fluorescence XAFS spectra (fluorescence intensity in arbitrary units vs. incident X-ray photon energy) for HgO, HgSCN, HgS, and $HgCl_2$. Each spectrum is unique to the respective compound. Spectra are offset vertically in increments of 0.15 for ease of visual examination.

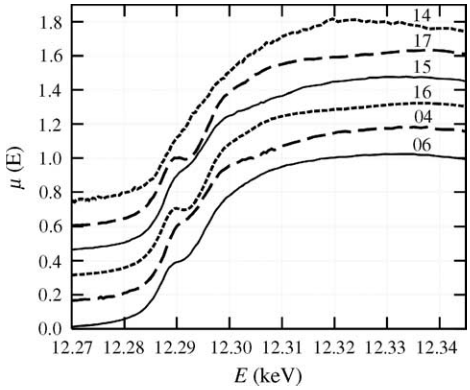

Fig. 2. Hg L_{III} fluorescence XAFS spectra (fluorescence intensity in arbitrary units vs. incident X-ray photon energy) for 1000 ppm Hg in water and simulant. The spectra for samples 04 and 15 are indistinguishable, as are the spectra for samples 16 and 17. The spectra for samples 06 and 14 are unique. Note that the spectra are offset vertically in increments of 0.15 for ease of visual examination.

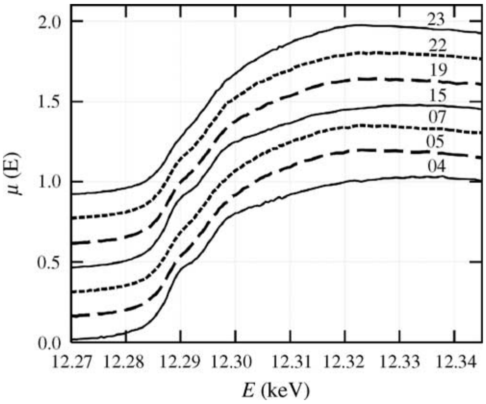

Fig. 3. Hg L_{III} fluorescence XAFS spectra (fluorescence intensity in arbitrary units vs. incident X-ray photon energy) for 1000 ppm Hg in simulant. The spectra for samples 04 and 15 are indistinguishable, as are the spectra for samples 05, 07, 19, 22, and 23. Note that the spectra are offset vertically in increments of 0.15 for ease of visual examination.

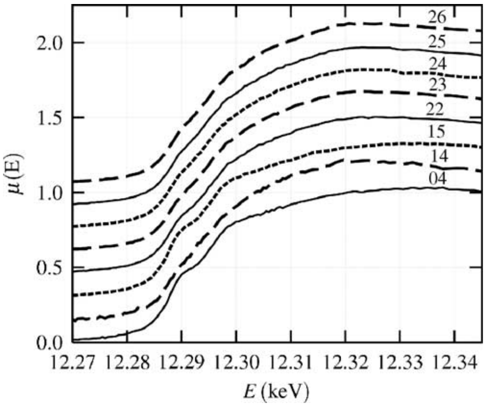

Fig. 4. Hg L_{III} fluorescence XAFS spectra (fluorescence intensity in arbitrary units vs. incident X-ray photon energy) for 1000 ppm Hg in simulant with various metals present. The spectra of samples 04 and 15 are indistinguishable, and the spectra for samples 14, 22, 23–26 are alike. Note that the spectra are offset vertically in increments of 0.15 for ease of visual examination.

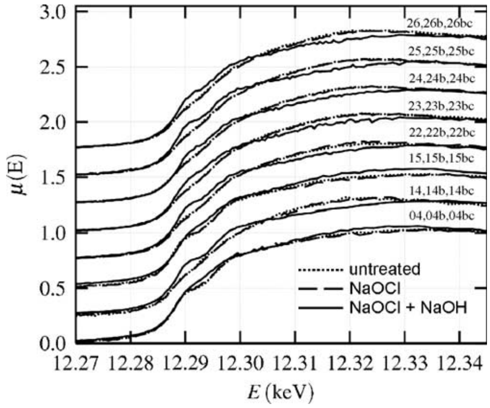

Fig. 5. Hg L_{III} fluorescence XAFS spectra (fluorescence intensity in arbitrary units vs. incident X-ray photon energy) for 1000 ppm Hg in simulant with various other metals present and sodium hypochlorite (designated by the label "b") or sodium hypochlorite plus sodium hydroxide (designated by the label "bc") added. The spectra for samples 04 and 15 are indistinguishable; the spectra for samples 04b, 04bc, 14bc, 15b, 15bc, 22bc, 23bc, 24bc, 25bc, and 26bc are alike; and the spectra for samples 14, 14b, 22, 22b, 23, 23b, 24, 24b, 25, 25b, 26, and 26b are the same. Note that the spectra from each family of samples, i.e., 4, 14, 15, 22–26, are offset vertically in increments of 0.25 for ease of visual examination.

simulant, Fig. 3 presents the effect that two iron sources have on mercury speciation in simulant, Fig. 4 demonstrates how co-contaminant metals affect mercury speciation in simulant, and Fig. 5 illustrates how sodium hypochlorite and sodium hydroxide affect mercury speciation in the presence of co-contaminant metals. Tables 2–5 provide a sample description and the spectral composition determined from fitting the measured XAFS spectra to a linear combination of spectra measured on standard Hg compounds.

The spectra for samples 04 and 15 in Fig. 2 are found to be essentially identical and the analysis shows that they have compositions consistent with one another. Similarly, the spectra for samples 16 and 17 are alike, and the best-fit combinations of model spectra give the same sample composition. The spectra and fitted compositions for samples 06 and 14 are both unique, and do not correspond to the spectra for any other samples presented in Fig. 2. With no other metals present, the speciation of mercury in mustard simulant is different than the speciation of mercury in water, as demonstrated by the spectra for samples 6 and 4 in Fig. 2. In water, the addition of Fe_2O_3 affects the speciation of mercury, but the addition of As_2O_3 to the iron/mercury-laden solution does not induce further change in mercury speciation, as shown by the spectra for samples 06, 16, and 17 in Fig. 2. Mercury is unaffected by the addition of Fe_2O_3 to simulant (see sample spectra 4 and 15 in Fig. 2). When As_2O_3 is added to simulant containing mercury and Fe_2O_3, however, the speciation of mercury is affected, as shown by the change that occurs in the spectra from sample 15 to 14. Regardless of whether mercury is alone, present with Fe_2O_3 or present with Fe_2O_3 and As_2O_3, the speciation of mercury in water and mercury in simulant is different.

Fig. 3 shows the effect that various iron sources and metals have on the XAFS spectra for mercury in simulant. The XAFS spectra (absorbed energy in arbitrary units versus incident X-ray photon energy) are offset vertically in increments of 0.15 for ease of visual examination. The spectra for samples 4 and 15 are indistinguishable and the spectra for samples 05, 07, 19, 22, and 23 are alike.

Fig. 3 and Table 3 show that in simulant, mercury is unaffected by the addition of Fe_2O_3 (comparing samples 04 and 15), but a change in the stable forms of mercury are induced upon addition of $FeSO_4$ (comparing samples 04 and 05) and upon the addition of cadmium and/or selenium (compare sample 04 to samples 07, 19, 22, and 23). The stable

Table 2
Composition of equilibrated samples in Fig. 2 as determined by fits of the XAFS spectra to linear combinations of spectra on model compounds

Sample	Description of initial components	Composition after equilibration period as determined by XAFS
06	Water + $HgCl_2$	$0.33HgCl_2 + 0.66HgSCN$
04	Thiodiglycol + $HgCl_2$	$0.25HgCl_2 + 0.75HgS$ (black)
16	Water + $HgCl_2$ + Fe_2O_3	$0.50HgCl_2 + 0.50HgSCN$
15	Thiodiglycol + $HgCl_2$ + Fe_2O_3	$0.25HgCl_2 + 0.75HgS$ (black)
17	Water + $HgCl_2$ + Fe_2O_3 + As_2O_3	$0.50HgCl_2 + 0.50HgSCN$
14	Thiodiglycol + $HgCl_2$ + Fe_2O_3 + As_2O_3	0.50HgSCN + 0.50HgS (black)

The resulting compositions typically have an uncertainty of 0.10 (i.e., 10%). While the compositions are suggestive of the actual Hg speciation, the reported values are best used to quantitatively compare spectra from different samples. Concentrations as in Table 1.

Table 3
Composition of equilibrated samples in Fig. 3 as determined by XAFS

Sample	Description of initial components	Composition after equilibration period as determined by XAFS
04	Thiodiglycol + $HgCl_2$	$0.25HgCl_2 + 0.75HgS$ (black)
05	Thiodiglycol + $HgCl_2$ + $FeSO_4$	0.50HgSCN + 0.50HgS (black)
19	Thiodiglycol + $HgCl_2$ + $FeSO_4$ + $CdCl_2$	0.50HgSCN + 0.50HgS (black)
07	Thiodiglycol + $HgCl_2$ + $FeSO_4$ + $CdCl_2$ + H_2SeO_3	0.50HgSCN + 0.50HgS (black)
15	Thiodiglycol + $HgCl_2$ + Fe_2O_3	$0.25HgCl_2 + 0.75HgS$ (black)
22	Thiodiglycol + $HgCl_2$ + Fe_2O_3 + $CdCl_2$	0.50HgSCN + 0.50HgS (black)
23	Thiodiglycol + $HgCl_2$ + Fe_2O_3 + $CdCl_2$ + H_2SeO_3	0.50HgSCN + 0.50HgS (black)

Concentrations as in Table 1.

Table 4
Composition of equilibrated samples in Fig. 4 as determined by XAFS

Sample	Description of initial components	Composition after equilibration period as determined by XAFS
04	Thiodiglycol + $HgCl_2$	$0.25HgCl_2 + 0.75HgS$ (black)
14	Thiodiglycol + $HgCl_2 + Fe_2O_3 + As_2O_3$	$0.50HgSCN + 0.50HgS$ (black)
15	Thiodiglycol + $HgCl_2 + Fe_2O_3$	$0.25HgCl_2 + 0.75HgS$ (black)
22	Thiodiglycol + $HgCl_2 + Fe_2O_3 + CdCl_2$	$0.50HgSCN + 0.50HgS$ (black)
23	Thiodiglycol + $HgCl_2 + Fe_2O_3 + CdCl_2 + H_2SeO_3$	$0.50HgSCN + 0.50HgS$ (black)
24	Thiodiglycol + $HgCl_2 + Fe_2O_3 + CdCl_2 + As_2O_3$	$0.50HgSCN + 0.50HgS$ (black)
25	Thiodiglycol + $HgCl_2 + As_2O_3$	$0.50HgSCN + 0.50HgS$ (black)
26	Thiodiglycol + $HgCl_2 + Fe_2O_3 + CdCl_2 + H_2SeO_3 + As_2O_3$	$0.50HgSCN + 0.50HgS$ (black)

Concentrations as in Table 1.

forms for mercury in samples 05, 19, 07, 22, and 23 are indistinguishable, with spectra that are consistent with half of the mercury as HgSCN and half as HgS (black).

The data in Fig. 4 contain the Hg L_{III} fluorescence XAFS spectra for mercury in mustard agent simulant with various co-contaminant metals present. The XAFS spectra (fluorescence intensity in arbitrary units versus incident X-ray photon energy) are offset vertically in increments of 0.15 for ease of visual examination. In Fig. 4, the spectra for samples 04 and 15 are alike, and the spectra for samples 14, 22, 23, 24, 25, and 26 are indistinguishable. Table 4 reveals the composition of the mercury in the samples after 10 months of equilibration as determined by XAFS.

Several observations can be derived from the spectra shown in Fig. 4 and the data presented in Table 4. As mentioned earlier, the presence of Fe_2O_3 alone does not influence mercury speciation in simulant (see spectra for samples 04 and 15). However, the addition of other metals, especially cadmium and arsenic, changes the stable form of mercury present in simulant. With mercury alone or mercury and Fe_2O_3 present, the mercury speciation is most consistent with a mixture of $HgCl_2$ and HgS (black). When other metals are added, the mercury spectra are most consistent with a mixture of HgSCN and HgS (black).

The XAFS spectra in Fig. 5 and the results in Table 5 demonstrate the effect of sodium hypochlorite addition and sodium hypochlorite plus sodium hydroxide addition on the state of mercury in thiodiglycol solutions with or without co-contaminant metals present. In Fig. 5, the XAFS spectra (fluorescence intensity in arbitrary units versus incident X-ray photon energy) are offset vertically in increments of 0.25 for ease of visual examination.

In the sample spectra presented in Fig. 5, three groups can be identified. Spectra for samples 04 and 15 are indistinguishable; mercury in these samples is most likely present as a combination of $HgCl_2$ and HgS (black). The spectra for samples 14, 14b, 22, 22b, 23, 23b, 24, 24b, 25, 25b, 26, and 26b also are indistinguishable, with the mercury speciation best fit by a mixture of HgSCN and HgS (black). The mercury in samples 04b, 04bc, 14bc, 15b, 15bc, 22bc, 23bc, 24bc, 25bc, and 26bc seems to be primarily in the form of HgS.

These classifications lead to several observations. First, the presence of bleach does not affect the mercury speciation if cadmium or arsenic is present (see samples 14, 14b, 22, 22b, 23, 23b, 24, 24b, 25, 25b, 26, and 26b). Second, the addition of caustic to the aforementioned samples changes the stable form of mercury, most likely from a combination of HgSCN and HgS (black) to primarily HgS (black). Finally, the addition of bleach to solutions containing either simulant and mercury (sample 04) or simulant, mercury, and Fe_2O_3 (sample 15) changes the stable form of mercury from a speciation that is consistent with a mixture of $HgCl_2$ and HgS

Table 5
Composition of equilibrated samples in Fig. 5 as determined by XAFS

Sample[a]	Description of initial components
04, 04b, 04bc	Thiodiglycol + $HgCl_2$
14, 14b, 14bc	Thiodiglycol + $HgCl_2 + Fe_2O_3 + As_2O_3$
15, 15b, 15bc	Thiodiglycol + $HgCl_2 + Fe_2O_3$
22, 22b, 22bc	Thiodiglycol + $HgCl_2 + Fe_2O_3 + CdCl_2$
23, 23b, 23bc	Thiodiglycol + $HgCl_2 + Fe_2O_3 + CdCl_2 + H_2SeO_3$
24, 24b, 24bc	Thiodiglycol + $HgCl_2 + Fe_2O_3 + CdCl_2 + As_2O_3$
25, 25b, 25bc	Thiodiglycol + $HgCl_2 + As_2O_3$
26, 26b, 26bc	Thiodiglycol + $HgCl_2 + Fe_2O_3 + CdCl_2 + H_2SeO_3 + As_2O_3$

Sample	Composition after equilibration period as determined by XAFS
04, 15	$0.25HgCl_2 + 0.75HgS$ (black)
14, 14b, 22, 22b, 23, 23b, 24, 24b, 25, 25b, 26, 26b	$0.50HgSCN + 0.50HgS$ (black)
04b, 04bc, 14bc, 15b, 15bc, 22bc, 23bc, 24bc, 25bc, 26bc	>0.90HgS (black)

Concentrations as in Table 1.
[a] b = NaOCl added; bc = NaOCl + NaOH added.

(black) to one that is primarily HgS (black). Further addition of caustic does not affect the prevalent form of mercury in these samples.

4. Conclusion

Overall, mercury speciates in water differently than it speciates in the mustard chemical warfare agent simulant, thiodiglycol. Limited samples of mercury in water and in thiodiglycol spiked with Fe_2O_3, As_2O_3, or both metals show that regardless of the spiking metal or combination of metals, the stable mercury species in water are different than they are in simulant. The addition of part per million levels of various metals such as arsenic and cadmium and the addition of bleach and caustic together influence the stable compounds of mercury formed. If mercury is to be precipitated or removed from liquid mustard prior to incineration processes, then several observations should be heeded. The behavior of mercury in water is much different than its behavior in simulant. Process chemistry treatment design parameters should not rely on speciation diagrams of mercury in water to predict the chemistry of mercury in agent, nor should design parameters ignore other metals present in solution. Our limited studies show that the concentration and forms of other metals in solution should be ascertained, and the concentration of added bleach and caustic should be noted prior to developing a correct mercury speciation/stabilization diagram.

Acknowledgements

Use of the Advanced Photon Source is supported by the U.S. Department of Energy, Office of Science, Office of Basic Energy Sciences, under Contract No. W-31-109-ENG-38. The authors thank the staff of GSECARS for their assistance in this project. We appreciate the efforts of Mr. Patrick Wilkey, Dr. Starnes Walker III, Dr. Harvey Drucker, and Mr. Alan Foley, all of ANL, for support in this effort.

References

[1] L. Ember, Chem. Eng. News 82 (2004) 8.
[2] Technical Secretariat for the Organisation for the Prohibition of Chemical Weapons, Convention on the Prohibition of the Development, Production, Stockpiling and Use of Chemical Weapons and on their Destruction, 1993.
[3] N.M. Munro, et al., Environ. Health Perspect. 107 (1999) 933.
[4] K.H. Nam, S. Gomez-Salazar, L.L. Tavlarides, Ind. Eng. Chem. Res. 42 (2003) 1955.
[5] R.W. Peters (Ed.), Separation of Heavy Metals and Other Trace Contaminants (AIChE Symposium Series), vol. 243, 1985, pp. 165–203.
[6] I. Wagner-Dobler, H. Von Canstein, Y. Li, K.N. Timmis, W.-D. Deckwer, Environ. Sci. Technol. 34 (2000) 4628.
[7] C.S. Krivanek III, J. Hazard. Mater. 47 (1996) 119.
[8] J.H. Pavlish, et al., Fuel Process. Technol. 82 (2003) 89.
[9] S.D. Faust, O.M. Aly, Chemistry of Water Treatment, second ed., CRC Press, Boca Raton, 1999, p. 402.
[10] C.S. Kim, G.E. Brown Jr., J.J. Rytuba, Sci. Total Environ. 261 (2000) 157.
[11] C.S. Kim, J.J. Rytuba, G.E. Brown Jr., J. Colloid Interface Sci. 271 (2004) 1.
[12] C.S. Kim, J.J. Rytuba, G.E. Brown Jr., J. Colloid Interface Sci. 271 (2004) 9.
[13] A.R. Lennie, J.M. Charnock, R.A.A. Pattrick, Chem. Geol. 199 (2003) 199.
[14] L.R. Skubal, et al., The examination of mercury interactions with iron in the presence of chemical agent simulant using EXAFS and XANES, Advanced Photon Source User Activity Report, Argonne, IL, 2004.